

Anti-Corrosion Inhibition of Mild Steel in 1M Hydrochloric Acid solution by using *Tiliacora acuminate* leaves Extract

R. Karthik^{1,2}, P. Muthukrishnan³, Shen-Ming Chen^{1,*}, B. Jeyaprabha⁴, P. Prakash^{2,*}

¹ Department of Chemical Engineering and Biotechnology, National Taipei University of Technology, Taipei, Taiwan 106 (ROC)

² Department of Chemistry, Thiagarajar College, Madurai-625009, India

³ Department of Chemistry, Faculty of Engineering, Karpagam University, Coimbatore-641021, India.

⁴ Department of Civil Engineering, Fatima Michael College of Engineering & Technology, Madurai-625 020, India.

*E-mail: smchen78@ms15.hinet.net; kmpprakash@gmail.com

Received: 18 December 2014 / Accepted: 25 February 2015 / Published: 23 March 2015

Anticorrosion activity of *Tiliacora acuminate* leaf extract (TALE) as a corrosion inhibitor in 1M HCl has been investigated using mass loss, potentiodynamic polarization, electrochemical impedance spectroscopy (EIS), scanning electron microscopy (SEM), UV-Visible spectroscopy and X-ray diffraction (XRD) studies. The mass loss results show that TALE is an excellent corrosion inhibitor. The inhibition efficiency increases with increasing the temperature from 308 to 333 K, reaching a maximum value of 93.02 % at the highest concentration of 320 ppm at the temperature of 333 K. Polarization measurements demonstrate that the TALE acts as a mixed type inhibitor. Nyquist plot illustrates that on increasing TALE concentration, the charge transfer increases and the double layer capacitance decreases. The adsorption of TALE on mild steel obeys Langmuir adsorption isotherm. SEM studies confirm the adsorption of TALE on mild steel surface.

Keywords: corrosion, metal, polarization, *Tiliacora acuminate*, SEM, XRD

1. INTRODUCTION

The use of inhibitors is one of the most practical methods for protection against corrosion, particularly in acidic media. Different organic and inorganic inhibitors have been used in prevention methods. These compounds have shown good anticorrosive activity but most of them are highly toxic to both human beings and the environment. Such inhibitors may cause reversible (temporary) or irreversible (permanent) damage to organ system viz., kidneys or liver, or to interrupt a biochemical

process or to disturb an enzyme system at some site in the body. The toxicity may manifest either during the synthesis of the compound or during its applications. Although the most effective and efficient organic inhibitors are compounds that have π bonds, the biological toxicity of these products, especially organic phosphate, is documented specifically about their environmental harmful characteristics [1]. The safety and environmental effects of corrosion inhibitors in industries have been always a global concern. Currently the use of natural products as corrosion inhibitor is gaining momentum to protect the metal against corrosion in aggressive acid solution. From the standpoint of safety, the development of non-toxic and effective inhibitors is considered more important and desirable, nowadays, which are also called eco-friendly or green corrosion inhibitors [2-12].

These toxic effects have led to the use of natural products as anticorrosive agents which are eco-friendly and harmless. In recent days many alternative eco-friendly corrosion inhibitors have been studied and prepared [13]. In this work, a plant extract called *Tiliacora acuminata* (TALE) has been used as a corrosion inhibitor. TALE is largely available in India. It belongs to Menispermaceae family. This plant has been used as an ingredient in many of the Ayurvedic preparations and regarded as an antidote for snake bite [14]. In the present study, the adsorption and the corrosion inhibition effect of TALE leaf extract has been investigated using mass loss, potentiodynamic polarization, electrochemical impedance spectroscopy (EIS), scanning electron microscopy (SEM), Fourier transform infrared spectroscopy (FT-IR), X-ray diffraction studies (XRD) and UV-visible analysis.

2. EXPERIMENTAL

2.1. Material Preparation

Mild steel (MS) specimens containing the composition (wt%): 0.05% C, 0.03% Si, 0.39% Mn, 0.60% P, 0.36% S and Fe balance were prepared for the size of 2.5cm length, 2.5cm breadth and 0.4cm of thickness which were polished with different emery papers ranging from 400 to 1200 grades followed by washing with acetone and dried at room temperature.

2.2. Test Solutions

The solution of 1M hydrochloric acid (Test solution) was prepared for each experiment using analytical grade of hydrochloric acid (98%) and diluted with distilled water. The concentration range of inhibitor was 200 to 320 ppm.

2.3. Preparation of TALE

The leaves were collected in Alagar Kovil, Madurai District, Tamil Nadu, India. The leaves were cut into small pieces, dried under shade conditions for 7 days and ground into fine powder. 10g of dried powder was extracted with absolute ethanol in Soxhlet apparatus for 3h. After completion of extraction, the extract was filtered and heated on a water bath at 55°C until most of the ethanol

evaporated. From the respective stock solutions, inhibitor solutions were diluted to desired concentrations for corrosion tests.

2.4. Methods

2.4.1. Mass loss method

The mass loss (ML) method is probably the most widely used method of inhibition assessment. Mass loss measurements were conducted under total immersion using 100ml capacity beakers containing 100ml test solution at 308 – 333K maintained in a thermostated water bath. The temperature maintenance in all immersion was 2 h. After 2h, the specimens were taken out from the test solution, washed thoroughly with distilled water followed by acetone, dried with air and polished with emery paper. The mass loss of mild steel specimens was determined by using an analytical balance with precision 0.1 mg. From the mass loss, the corrosion rates (CR) were calculated as follows:

$$CR_{(mpy)} = 534 \times (W_b - W_a) / DST \quad (1)$$

Where W_b and W_a are the specimen mass before and after immersion in the test solution respectively, D is the density of iron ($7.8\text{g}\cdot\text{cm}^{-3}$), S is the surface area of the specimen in cm^2 and T is the period of immersion in hours.

2.4.2 Potentiodynamic polarization measurements

Potentiodynamic polarization studies were carried out using H & CH electrochemical workstation impedance Analyzer Model CHI 604D. Mild steel was used as a working electrode. Platinum electrode and Saturated Calomel Electrode were used as counter electrode and a reference electrode respectively. The working electrode was made from a commercial grade of mild steel sheet insulated with Araldite. The area exposed to the acid solution was 1cm^2 . Before measurement the electrode was immersed in the test solution at open circuit potential (OCP) for 30min to be sufficient to reach a stable state. Potentiodynamic polarization curves were recorded from -300 to +300 mV_{SCE} , (versus OCP). All electrochemical measurements were carried out at 308K using 100ml of electrolyte (1M HCl) in a stationary condition. Each experiment was repeated at least three times to determine the reproducibility.

The corrosion parameters such as corrosion potential (E_{corr}), corrosion current (I_{corr}) and Tafel slopes (b_c and b_a) were measured. During the polarization study, the scan rate (V/s) was 0.001; Hold time at E_f (s) was zero and quiet time (s) was 2.

2.4.3. Electrochemical impedance measurement

AC impedance spectra were recorded in the same instrument used for polarization study using three-electrode cell assembly. The real part and imaginary part of the cell impedance were measured in

ohms for various frequencies. The charge transfer resistance (R_{ct}) and double layer capacitance (C_{dl}) values were computed [15].

$$R_{ct} = (R_s + R_{ct}) - R_s \quad (2)$$

$$C_{dl} = \frac{1}{2} \cdot \pi R_{ct} f_{max} \quad (3)$$

Where R_s = solution resistance, f_{max} = maximum frequency. AC impedance were recorded with initial E (v) = 0 values; High frequency (Hz) = 1×10^5 , Low frequency (Hz) = 0.1; Amplitude (v) = 0.005 and Quiet time (s) = 2.

2.4.4. FT-IR spectroscopy and X-ray diffraction studies

The nature of the protective film formed on the surface of the mild steel in 1M HCl in the presence of the inhibitor (320ppm TALE) for a period of 2 h was studied. After 2 h, the specimens were taken out and dried. The film between metal/solution interfaces was analyzed by using FT-IR spectroscopy (8400S SHIMADZU spectrometer) and X-ray diffractometer, Model (X' pert Pro PANalytical, Netherland).

2.4.5. Scanning Electron Microscopy (SEM)

The mild steel specimens were immersed for 2h in 1M HCl solution containing optimum concentrations (320 ppm TALE) of inhibitor. After 2 h, the specimens were taken out and dried. The surface morphology of the mild steel was examined by using the JEOL (JSM 6390) Scanning electronic microscope.

2.4.6. UV-Visible spectroscopic studies

TALE treated with 1M HCl and after 2h mild steel immersion were analyzed using JASCOW 32 spectrophotometer. The absorption spectra of these solutions were determined with test solution as a reference.

3. RESULTS AND DISCUSSION

3.1. Evaluation of TALE as Corrosion Inhibitor in 1M HCl Solutions

Based on the ML measurements, CR and IE_w % for various concentrations of TALE leaves extract, after 2 h of immersion at the temperatures of 308K, 313K, 323K and 333K are given in Fig 1. The following equation was used to determine the inhibition efficiency (IE_w %):

$$IE_w \% = \frac{CR_0 - CR_{inh}}{CR_0} \times 100 \quad (4)$$

Where CR_0 and CR_{inh} are the corrosion rates of MS in the absence and presence of inhibitor. It can be observed that the values of IE_w % gradually increase with the increase in concentration of TALE, reaching a maximum value of 93.02 % at the highest concentration of 320 ppm at the

temperature of 333 K. With increase in temperature from 308 K to 333 K, there is an increase in the value of IEw% which may be attributed to the strong adsorption of some additive molecules (Fig.1). This result suggests that there should be strong chemical bonding between the TALE and the mild steel surface [16]. From the study, it is confirmed that the inhibitor effectively protects the MS even at high temperatures.

The degree of surface coverage θ at different concentrations of the additive in acidic medium has been evaluated from ML using the equation

$$\theta = \frac{CR_0 - CR_{inh}}{CR_0} \tag{5}$$

From Fig 2, it is observed that the increase in the value of CR_0 is more pronounced with the rise in temperature of the blank acid solution. In the presence of TALE, the corrosion rate value decreases with increase in temperature, which is caused by the strong adsorption of extract molecules on the MS surface. The increase in the area of surface coverage also suggests that TALE strongly adsorbs on the metal surface. The results show that the TALE can effectively protect the MS even at high temperatures.

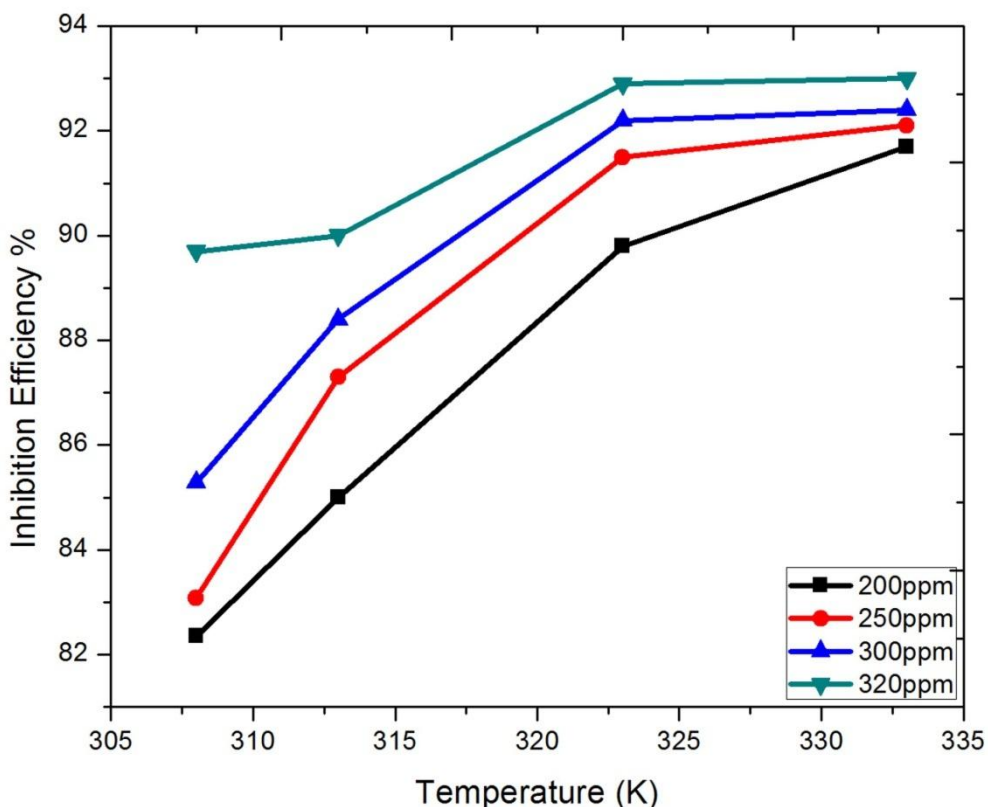


Figure 1. Variation of inhibition efficiency of TALE with temperature

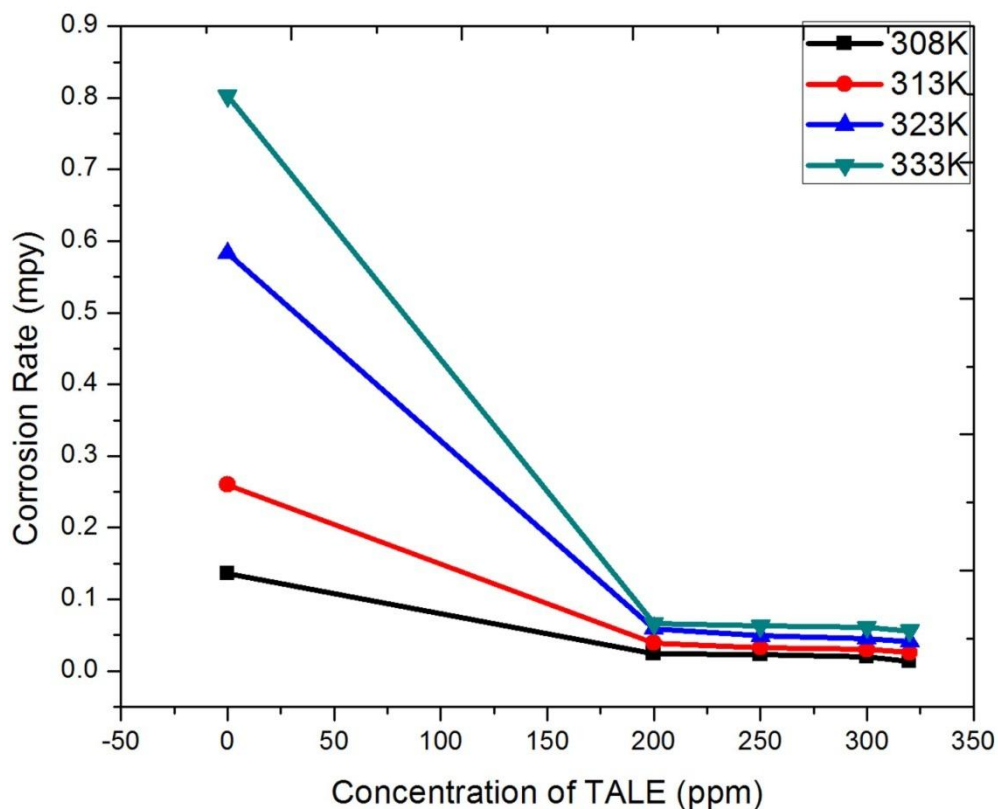


Figure 2. The relationship between corrosion rate and concentration (ppm) for different temperature of TALE

3.2. Thermodynamic activation parameters

Temperature is an important parameter in the studies of metal dissolution. The effect of temperature on the inhibited acid-metal reaction is very complex because many changes may occur on the metal surface such as rapid etching, desorption of inhibitor and the inhibitor may undergo decomposition.

The dependence of corrosion rate on temperature can be conveyed by the Arrhenius equation

$$\log CR = \log \lambda - (E_a / 2.303RT) \tag{6}$$

Where, CR is the corrosion rate, T is the absolute temperature, E_a is the apparent activation energy, R is the molar gas constant and λ is the frequency factor. A plot of log of CR obtained from gravimetric measurements versus $1/T$ gives a straight line with a regression coefficient close to unity (Fig. 3). The values of apparent activation energy (E_a) and pre exponential factor were calculated from the slope and intercept of the straight lines obtained in Arrhenius plot and the results are given in Table 1.

The data indicate that the thermodynamic activation energy (E_a) of the corrosion of mild steel in 1M HCl in the presence of TALE is less than that in the free acid solution. This finding indicates that TALE retards the corrosion of mild steel in the examined medium. The value of E_a is lower for

the inhibited solution than for the uninhibited solution. Generally lower E_a value leads to the lower corrosion rate.

The transition state equation is given as

$$\log CR/T = \{ \log(R/hN) + (\Delta S^*/2.303R) \} - (\Delta H^*/2.303RT) \tag{7}$$

Where, h is Planck's constant, N is Avogadro's number, ΔS^* the entropy of activation and ΔH^* is the enthalpy of activation. A plot of $\log CR/T$ versus $1/T$ gives a straight line (Fig.4) with a slope of $-\Delta H^*/2.303R$ and the intercepts of $\log R/hN + \Delta S^*/2.303$, the values of ΔS^* and ΔH^* were calculated and listed in Table 1. The positive sign of enthalpies reflects the endothermic nature of the steel dissolution process meaning that the dissolution of steel is difficult. The positive values of the entropy of activation both in the absence and the presence of the inhibitor imply that the activated complexes in the rate determining step represent an association rather than a dissociation step, meaning that decrease in disordering takes place on going from reactants to the activated complexes.

Table 1. Activation parameters of the dissolution of mild steel in 1M HCl in the absence and presence of different concentration of TALE

Acid solution	Concentration of inhibitors	E_a (kJ/mol)	ΔH^* (kJ/mol)	$-\Delta S^*$ (J/mol/K)
1M HCl	0	53.87	58.23	71.81
	200	33.22	31.24	173.73
	250	33.43	31.47	173.94
	300	36.64	34.90	163.95
	320	44.65	42.79	140.64

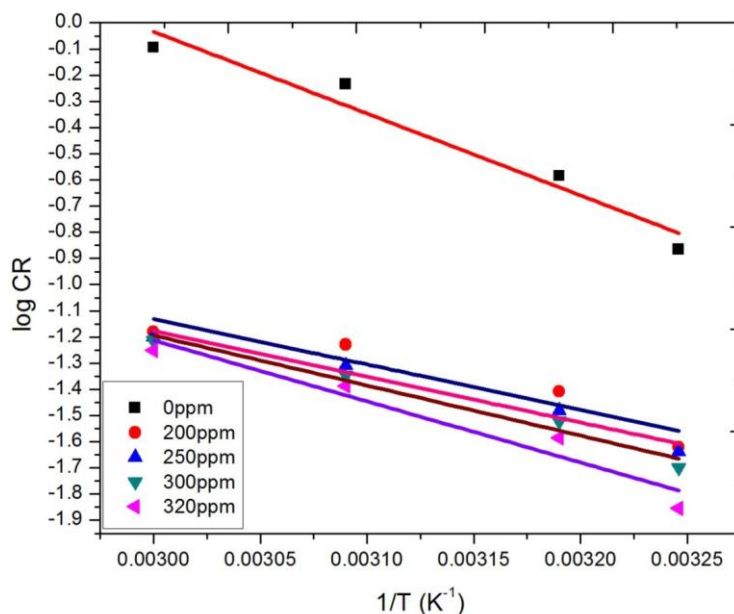


Figure 3. Arrhenius plot for mild steel corrosion in 1M HCl in the absence and presence of different concentration of TALE.

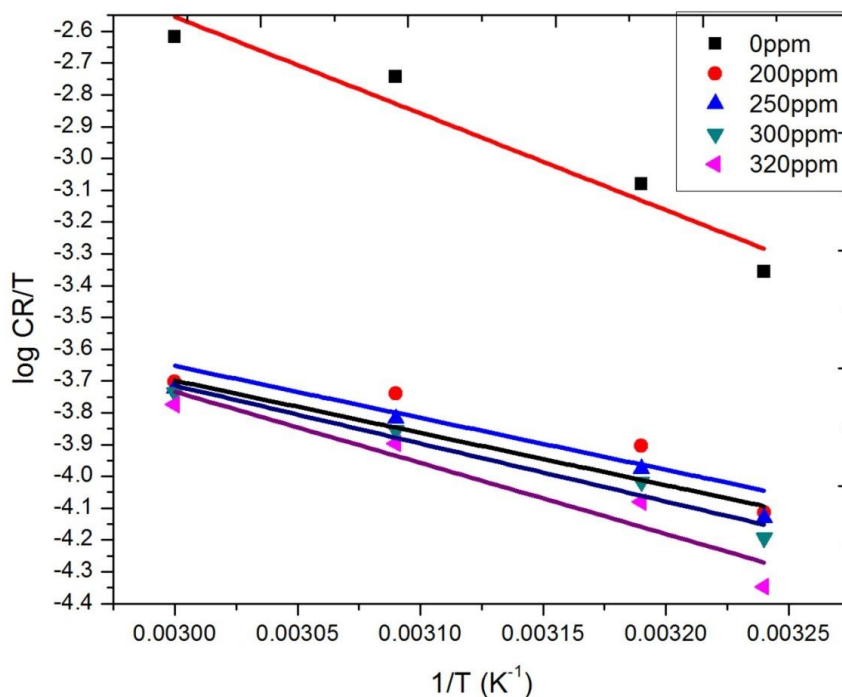


Figure 4. Transition state plot for mild steel corrosion in 1M HCl in the absence and presence of different concentration of TALE

3.3. Adsorption isotherm

The adsorption of the inhibitor is influenced by the nature and the charge of the metal, the chemical structure of the inhibitor, distribution of the charge in the molecule and the type of electrolyte [17-20]. Important information about the interaction between the inhibitor and steel surface can be furnished by the study of adsorption isotherm. In the present work, it is found that θ increases with the inhibitor concentration, which is attributed to more adsorption of inhibitor molecules on to the MS surface. If the adsorption of TALE is assumed to belong to a monolayer adsorption, the Langmuir adsorption isotherm can be applied to investigate the mechanism by the following equation:

$$C/\theta = \frac{1}{K} + C \tag{8}$$

Where C is the inhibitor concentration in the electrolyte and K_{ads} is the equilibrium constant for the adsorption/desorption process. The surface coverage (θ) values were calculated using mass loss data at 308-333K for mild steel in 1M HCl with various concentrations of extract and the values of C/ θ was plotted against C as shown in Fig.5. These plots are linear with a slope equal to unity. The value of K_{ads} is related to the standard free energy of adsorption, ΔG^0_{ads} by the following equation,

$$\Delta G^0_{ads} = - RT \ln (55.5 \times K_{ads}) \tag{9}$$

Where, R is the gas constant, T is the Absolute temperature. The value of 55.5 is the molar concentration of water in solution expressed in mol⁻¹ concentration. The correlation coefficient (R^2)

was used to choose the adsorption isotherm that best fits the experimental data and it is found that the adsorption process follows the Langmuir adsorption isotherm ($R^2 > 0.99$). The other isotherms viz. Temkin and Freundlich isotherms do not fit the data significantly. The calculated thermodynamic adsorption parameters are listed in Table 2. The negative values of ΔG^0_{ads} suggest that the adsorption of the TALE extract on the mild steel surface is spontaneous. Generally, ΔG^0_{ads} values between 0 and -20kJ/mol are associated with electrostatic interactions between the charged molecules and charged metal surface (physisorption). The values of ΔG^0_{ads} around -40kJ mol⁻¹ or more negative involve charge sharing or transfer of charge from the inhibitor molecules to the metal surface to form a coordinate-covalent bond, (chemisorptions) [21-23]. In this work, ΔG^0_{ads} values are slightly less than -40kJ/mol, which indicates that the TALE extract adsorbed on steel surface involve physical and chemical adsorption [24-26].

Table 2. Thermodynamic parameters for adsorption of TALE on the Mild steel in 1M HCl

Acid solution	Temperature (K)	K_{ads}	ΔG^0_{ads} (kJ/mol)	R^2 (Langmuir)	R^2 (Temkin)	R^2 (Freundlich)
1M HCl	308	200	-23.85	0.998	0.734	0.727
	313	250	-24.82	1	0.929	0.907
	323	500	-27.47	1	0.937	0.917
	333	1000	-30.24	0.998	0.854	0.851

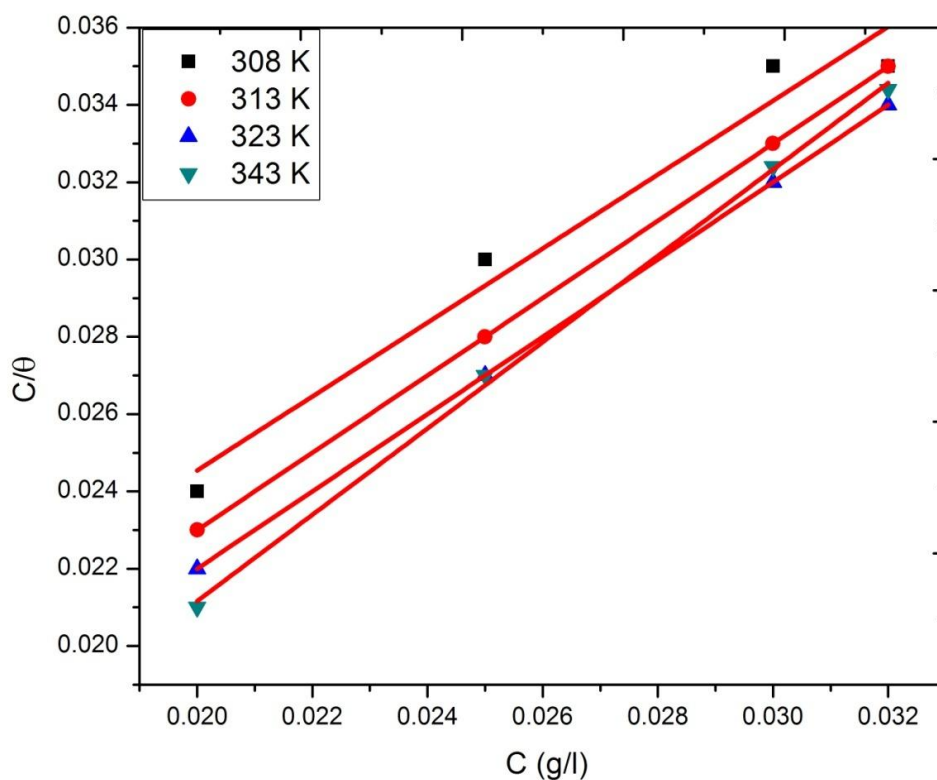


Figure 5. Langmuir adsorption plots of mild steel in 1M HCl solution containing different concentration of TALE.

3.4. Potentiodynamic polarization measurements

Fig. 6 shows the anodic and cathodic polarization curves of mild steel in 1M HCl solution in the absence and presence of TALE. From the figure, it is clear that the cathodic reactions of steel electrode corrosion are inhibited with the increasing TALE concentrations. Also, the addition of TALE has suppressed the cathodic reactions and anodic reactions. It means that the addition of TALE reduces the cathodic hydrogen evolution reaction and retards the anodic dissolution reaction, which suggests that the inhibitor acts as a mixed type inhibitor [27-29]. The values of b_a are shifted to lower values with reference to blank in the presence of TALE. At higher concentration (300ppm), the Tafel slopes values (b_c and b_a) increase in 1M HCl solutions. This shows that TALE inhibits the corrosion mechanism by controlling cathodic reactions predominantly and anodic sites of the metal surface [30]. From these values, it is confirmed that TALE acts as a mixed-type inhibitor. Electrochemical kinetic parameters such as corrosion potential (E_{corr}), cathodic and anodic slope (b_c and b_a), corrosion current density (i_{corr}) and percentage of inhibition efficiency were obtained from Tafel curves and are given in Table 3.

The inhibition efficiency is defined as

$$IE\% = (i_{corr}^0 - i_{corr} / i_{corr}^0) \times 100 \tag{10}$$

Where i_{corr}^0 and i_{corr} are the corrosion current density values in the absence and presence of inhibitor respectively. Table 3. shows that the i_{corr} values decrease in the presence of inhibitor, which is due to the increase in the blocked fraction of the electrode surface by adsorption.

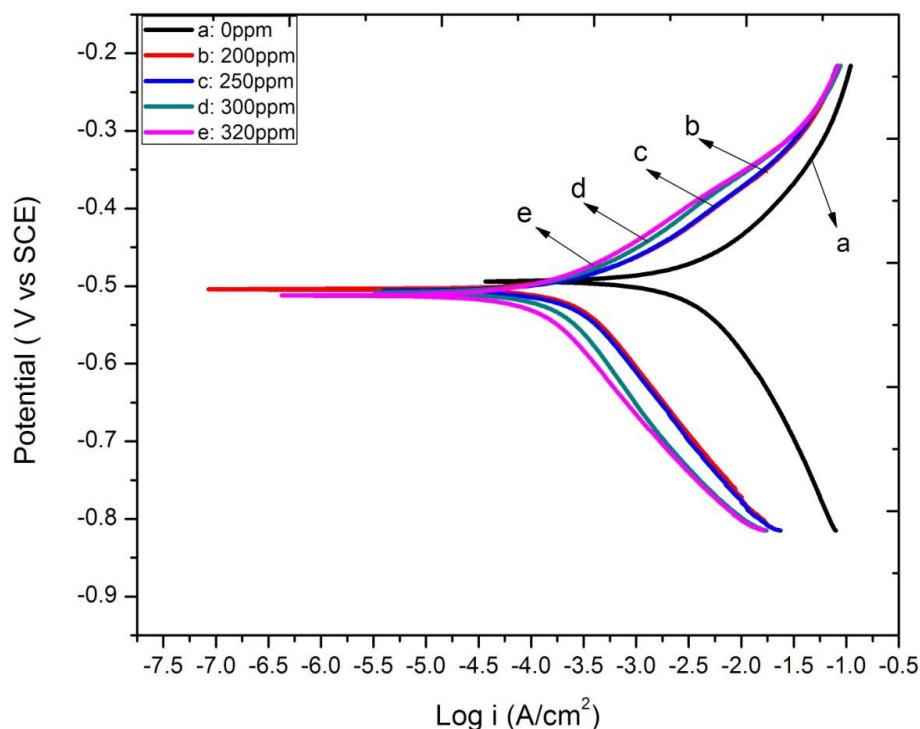


Figure 6. Potentiodynamic polarization curves for mild steel in 1M hydrochloric acid in the absence and presence of inhibitors.

Table 3. Effect of TALE on corrosion of MS in 1 M HCl solution studied by electrochemical polarizations methods

Concentration of inhibitor (ppm)	E_{corr} (V)	Tafel Constant (mV/decade)		I_{corr} (mA/cm ²)	IE %
		b_a (mV dec ⁻¹)	b_c (mV dec ⁻¹)		
0	-0.494	135.04	180.2	4310	-
200	-0.504	96.9	171.1	394	90.85
250	-0.506	96.0	170.3	364	91.55
300	-0.508	97.7	184.7	254	94.10
320	-0.512	90.8	164.0	161	96.26

3.5. Electrochemical Impedance measurements

Impedance diagrams obtained for mild steel in 1 M HCl in the presence and absence of the inhibitors are shown in Fig 7. The impedance parameters such as R_s , R_{ct} , C_{dl} and f_{max} derived from Nyquist plots are given in Table 4. The charge transfer resistance increases with increase in concentration of inhibitor in acid solution. In the impedance studies, IE% was calculated as:

$$\text{IE}\% = (R_{ct(\text{inh})} - R_{ct} / R_{ct(\text{inh})}) \times 100 \quad (11)$$

Where R_{ct} and $R_{ct(\text{inh})}$ are uninhibited and inhibited charge transfer resistance respectively. The diameter of Nyquist plots increases on increasing the concentration of TALE which indicates the strengthening of inhibitor film. As the concentration of inhibitor increases, charge transfer resistance enhances and decreases the double layer capacitance values. The decrease in C_{dl} is due to the gradual replacement of water molecules by the adsorption of inhibitor molecules at metal/solution interface, which leads to the formation of protective film on the mild steel surface and then it retards the extent of the dissolution reaction. The decrease in C_{dl} is attributed to a decrease in local dielectric constant and increase in thickness of the electrical double layer [31]. This is due to the adsorption of TALE on the metal surface leading to the formation of a protective layer on the electrode surface [32]. The use of natural products as corrosion inhibitors extracted from leaves have been widely reported [33-45]. Table 5 reports the percentage inhibition efficiency for some plant extracts used as corrosion inhibitors in various acidic media and their optimum concentrations. The comparison of data obtained by a lot of natural products (Table 5) with our results (Table 2, 3 and 4) suggests that the plant extract studied in the present work can serve as an effective corrosion inhibitor for MS corrosion.

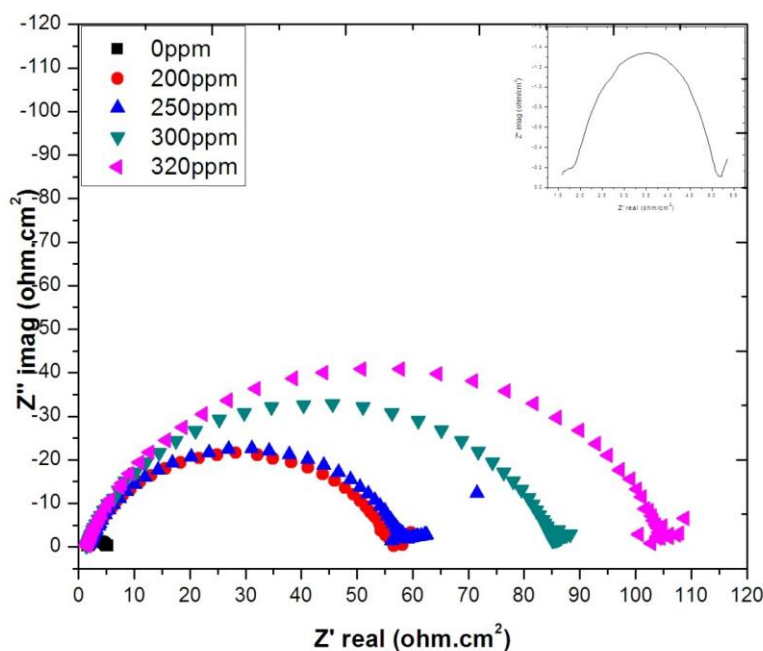


Figure 7. Nyquist diagram for mild steel in 1M HCl in the absence and presence of TALE extract

Table 4. Data from electrochemical impedance measurements for corrosion of MS in 1 M HCl solutions at various concentrations of TALE

Concentration of inhibitor (ppm)	R_s (Ohm.cm ²)	R_{ct} (Ohm.cm ²)	f_{max}	C_{dl} (μF/cm ²)	Inhibition Efficiency IE %
0	1.864	3.20	1	3.69×10^{-2}	-
200	0.683	56.18	22	1.31×10^{-4}	94.30
250	0.613	58.81	23	1.20×10^{-4}	94.55
300	0.553	86.28	33	5.64×10^{-5}	96.29
320	0.229	107.18	41	3.61×10^{-5}	97.01

Table 5. Percentage inhibition efficiency of different plants extracts at optimum concentration.

S.No	Natural products	Acid solution	Optimum concentration	Techniques			Metal exposed
				Mass loss	Tafel	EIS	
1	Aloe vera [30]	2M HCl	10%(v/v)	67 (313K)	-	-	Zinc
2	Euphorbia hirta[31]	0.5M HCl	0.25mg	97 (303K)	-	-	Al-alloy
3	Foeniculam vulgare[32]	1M HCl	3ml/l	66 (343K)	77	76	C-steel
4	Xylophia Ferraginea[33]	1M HCl	500ppm	-	87	82	Mild steel
5	Garcinia	HCl	25%(v/v)	96.3 (318K)	96.36	96.36	Mild steel

mangostana[34]							
6	Aq.garlic peel[35]	1M HCl	400mg/l	83 (328K)	90	98	C-steel
7	Gossipium hirsutum[36]	2M NaOH	52%(v/v)	-	-	97.04	Aluminum
8	a)Hyppocratea pallens	1M HCl	1000mg/l	95.8 (333K)	90.5	88.3	Mild steel
	b)Hyppocratea planch[37]	0.5M H ₂ SO ₄		93.3 (333K)	93.5	95	
9	Prunus cerasus[38]	1M HCl	4% (v/v)	81.02 (358K)	92.65	94	Steel
10	Mentha spicata[39]	1 M HCl	2g/l	63 (333K)	93	88	Steel
11	Musa acuminata[40]	1N HCl	1%(v/v)	86.42 (353K)	69.07	91.85	Mild steel
12	a)Kola plant	0.5M HCl	0.5 M	-	-	73.8	Mild steel
	b)Tobacco[41]					96.25	
13	Egg plant peel[42]	2M HCl	1000ppm	79.15 (323K)	62.4	81.7	Mild steel
14	Present Study	1M HCl	320ppm	93.5 (333K)	96.26	97.07	Mild steel

3.6. Scanning Electron Microscope (SEM)

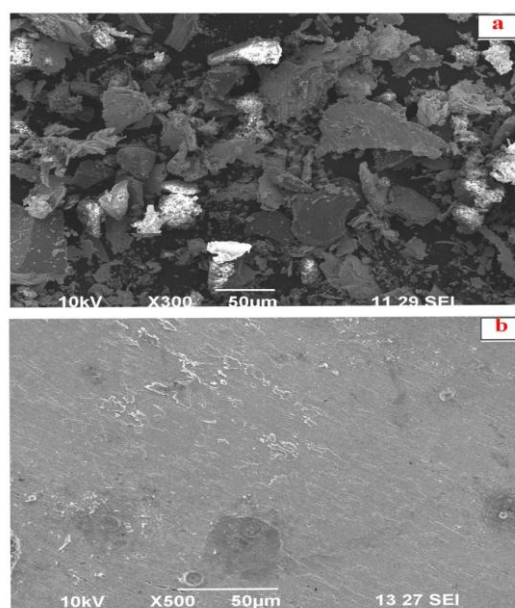


Figure 8. SEM images of mild steel in 1M hydrochloric acid (a) without inhibitor (b) with 320ppm of inhibitor.

Fig.8a shows the roughness of the metal surface which indicates the corrosion of mild steel in acid solution. Fig.8b shows the appearance of smooth mild steel surfaces after the addition of inhibitors to the acid solution. This examination indicates that corrosion rate is reduced in the presence of inhibitors. This is due to the adsorption of inhibitor molecules on the metal surface as a protective layer.

3.7. X-ray diffraction studies (XRD)

X-ray diffraction studies are used to determine film formation of mild steel in various test solutions. Peaks due to iron oxides (Fe_3O_4 and FeOOH) appear at $2\theta = 35.5^\circ$, 42.9° and 64.9° (Fig. 9A). This indicates that in the acid solution mild steel specimen has undergone corrosion leading to the formation of magnetite [46]. The XRD pattern of the surface of the mild steel immersed in the acid solution containing 320ppm of TALE is shown in Fig.9B. The iron peaks appear at $2\theta = 44.5^\circ$ and 82.2° . It is observed that the peaks due to oxides of iron such as Fe_3O_4 and FeOOH are found to be absent. This confirms that the metal is completely protected from corrosion and also the protective film does not consist of any oxide of iron [47-49].

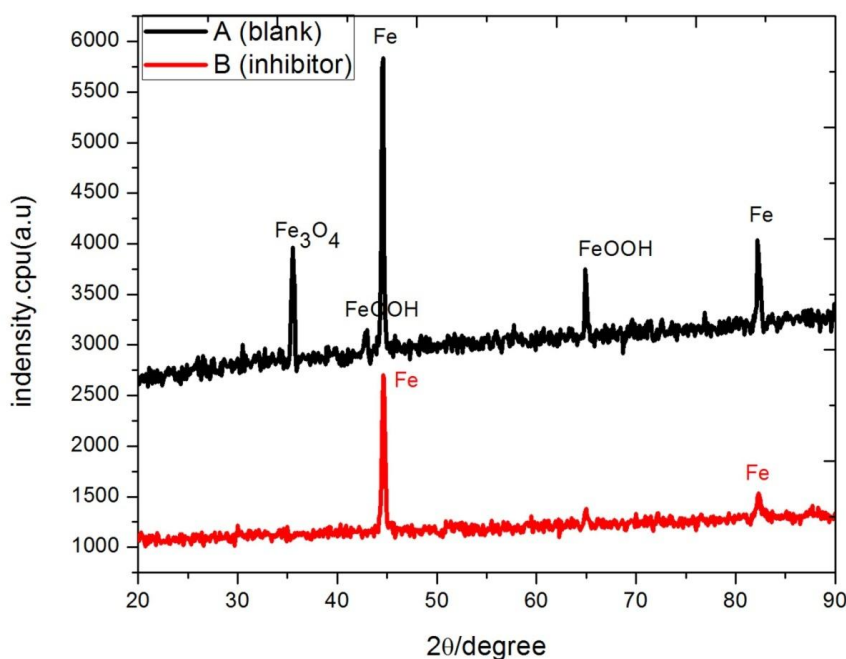


Figure 9. XRD spectrum of mild steel corrosion in the A) absence B) presence of TALE.

3.8. Analysis of FT-IR spectra

Earlier researchers have confirmed that FTIR spectrometer is a powerful instrument that can be used to determine the type of bonding and the nature of inhibitors adsorbed on the metal surface [50-51]. In order to evaluate the protective layer formed on the steel surface in the presence of inhibitors and also to provide new bonding information on the steel surface, FTIR study was carried out. The FT-

IR spectrum of TALE is given in Fig.10a. Broad band at 3316.6 cm^{-1} is observed in the spectrum of TALE extract indicates -OH or N-H stretching vibration. A peak observed at 1602.8 cm^{-1} is attributable for the aromatic -C=O- stretching frequency. The absorption band at 1425 cm^{-1} is due to C-H bending mode of CH_2 . The peak at 1068 cm^{-1} is due to the C-O-C stretching of ether compounds. The adsorption bands below 1000 cm^{-1} correspond to aliphatic and aromatic C-H group. The FTIR spectrum (KBr) of the film formed on the surface of the mild steel after immersion in acid solution with 320ppm of TALE is shown in Fig.10b. On comparing 10a and b, there is a downshift from 3316 to 3406 cm^{-1} , which is attributed to the change in the frequencies of hydroxyl and amino groups. The -C=O stretching frequency has increased from 1602 to 1628 cm^{-1} . This indicates that TALE has coordinated with Fe^{2+} through O atoms in -C=O stretching frequency. The result shows that TALE contains oxygen and nitrogen atoms in functional groups (O-H , N-H , C-O-C , C=O , C-H) and aromatic ring, which mainly bond with metal and protect mild steel from corrosion.

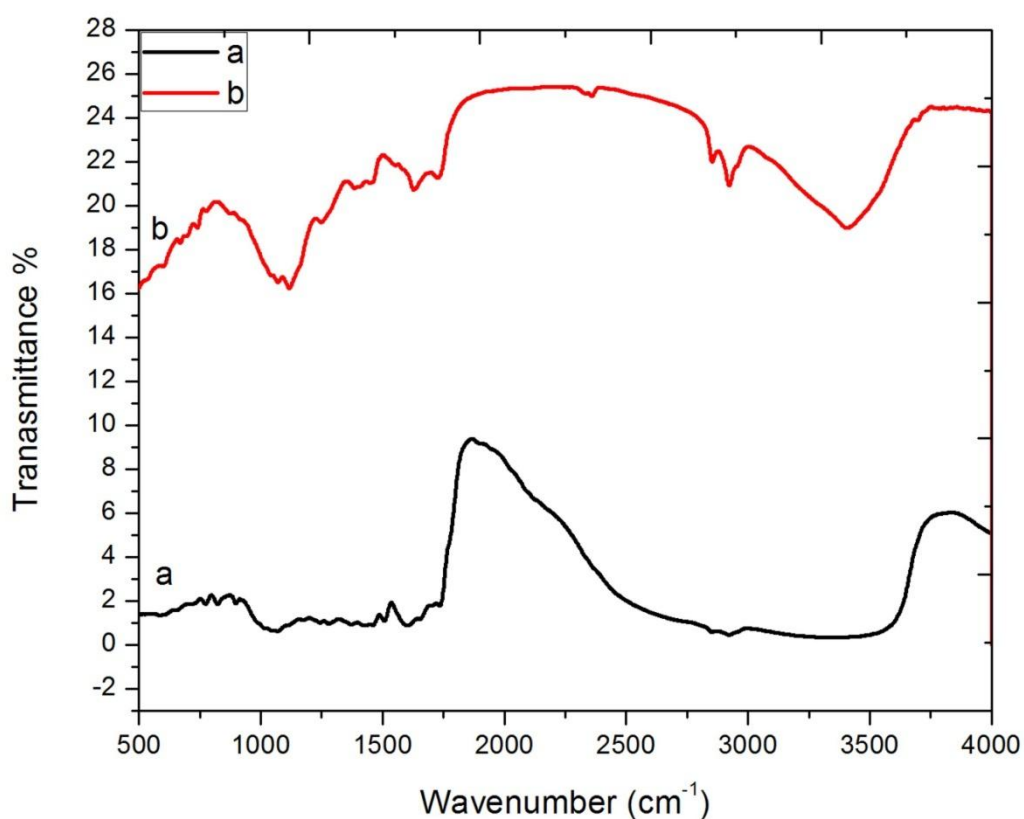


Figure 10. FT-IR spectra of (a) pure compounds, (b) adsorbed layer formed on the mild steel after immersion in 1M Hydrochloric acid solution containing inhibitors.

3.9. UV-visible analysis

In order to confirm the possibility of the formation of inhibitor-Fe complex, UV-Visible absorption spectra obtained from 1M HCl solution containing 320 ppm TALE before and after the mild steel immersion are shown in figure 11. The electronic absorption spectra of TALE before

immersion have absorption maximum at 214nm and 288nm, which can be attributed to π - π^* and n- π^* transitions. After 2hrs immersion of mild steel, the change in the position of absorption maximum or the change in the absorbance values indicates that the complex formation between two species in solution. However, there is no change in the shape of absorption spectra. These experimental findings provide the formation of complex between Fe^{2+} and TALE and confirm the inhibition of steel from corrosion.

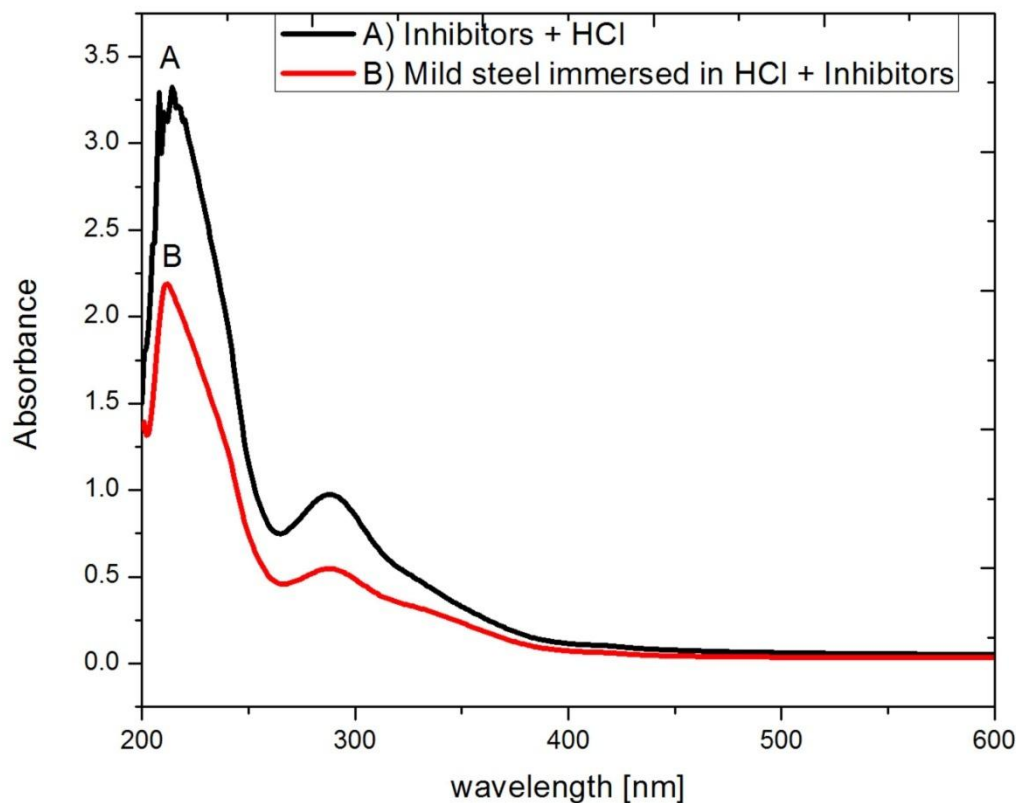


Figure 11. UV-visible spectra of the solution containing 1M HCl before (A) and after the mild steel immersion in inhibitor (B)

3.10. Mechanism of corrosion inhibition

From the results obtained from different electrochemical and mass loss measurements, it can be concluded that TALE inhibits the corrosion of mild steel in 1M HCl by adsorption at mild steel/solution interface. It is a general assumption that the adsorption of natural inhibitors at the metal surface interface is the first step in the mechanism of the inhibitor action. Natural molecules may be adsorbed on the metal surface in four ways [52] namely

- (a) Electrostatic interaction between the charged molecules and the charged metal,
- (b) Interaction of unshared electron pairs in the molecule with the metal,
- (c) Interaction of p-electrons with the metal and/or
- (d) A combination of types (a–c).

In general, TALE contains alkaloids, aminoacids, protein, carbohydrates, tannins, with the heteroatoms like N, O etc., which may act as reaction centers for the adsorption process. The inhibition of active dissolution of the metal is due to the adsorption of the inhibitor molecules on the metal surface forming a protective film. The inhibitor molecules can be adsorbed onto the metal surface through electron transfer from the adsorbed species to the vacant electron orbital of low energy in the metal to form a co-ordinate type link. The inhibition efficiency depends on many factors [53] including the number of adsorption centers, mode of interactions with metal surface, molecular size and structure. It is well known that iron has co-ordinate affinity toward nitrogen, sulfur and oxygen-bearing ligands [54-55]. Hence, adsorption on iron can be attributed to co-ordination through carbonyl linkage, hetero atom (N and O) and p-electrons of aromatic ring. There are unshared electron pairs on N and O which are capable of forming a coordination bond with iron. TALE is more effectively adsorbed. From all the above facts, it is confirmed that the investigated TALE follows type (d) mechanism.

4. CONCLUSION

The present work leads to the following conclusions:

- The inhibition efficiency of the studied inhibitor (TALE) increases with increasing temperature and increasing inhibitor concentrations.
- Polarization study reveals that the TALE acts as a mixed type inhibitor controlling both anodic and cathodic processes.
- An electrochemical impedance spectrum confirm the formation of protective layer on the mild steel surface.
- The adsorption of studied inhibitor obeys Langmuir adsorption isotherm at all temperatures (308-333K).
- ΔG values lies above -20kJ/mol , which shows that the adsorption is mixed type of adsorption. SEM and XRD image indicate the possibility of formation of the film on the surface and gives morphology of the mild steel surface.
- FT-IR spectra reveal that the inhibitor is adsorbed on the metal surface.

References

1. M.A .Amee and A.M.Fekry, *Prog Org. Coat.*, 71 (2011) 343.
2. J.C.D.Rocha, J.A.Da Cunha Ponciano Gomes and E.D.Elia, *Corros Sci.*, 52 (2010) 2341.
3. N.Lahhit, A.Bouyanze, J.M.Desjobert, B.Hammouti and R.Salghi, *Electrochimi Acta.*, 29 (2011) 127.
4. M.Dahmani, A.Et-Touham, S.S.Al-Deyab, B.Hammouti and A.Bouyanze, *Int J Electrochem Sci.*, 5 (2010) 1060.
5. B.Senhaj, I.Ben, D.Hmamou, R.Salghi and A.Zarrouk, *Int J Electrochem Sci.*, 8 (2010) 6033.
6. D.Ben Hmamou, R.Salghi, A. Zarrouk, B.Hammouti and S.S.Al-Deya, *Int J Electrochem Sci.*, 7 (2012) 2361.

7. N.S.Patel, S.Jauhari, G.N.Mehta, S.S.Al-Deyab and I.Warad, *Int J Electrochem Sci.*, 8 (2013) 2635.
8. D.Ben Hmamou, R.Salghi, L.Bazzi, B. Hammouti and S.S.Al-Deyab, *Int J Electrochem Sci.*, 7 (2012) 1303.
9. Z.Faska, A.Bellioua, M. Bouklah, L. Majidi and R.Fihi, *Monatshefte für Chemie.*, 139 (2008) 1417.
10. A.Ghazoui, N.Bencaht, S.S.Al-Deyab, A. Zarrouk and B.Hammouti, *Int J Electrochem Sci.*, 8 (2013) 2272.
11. A.Khadraoui, A.Khelifa, L.Touafri, H.Hamitouche and R.Mehdaoui, *J Mater Environ Sci.*, 4 (5) (2013) 663.
12. M.Boudalia, A.Guenbour, A.Bellaouchou, A.Laqhaili and M.Mousaddak, *Int J Electrochem Sci.*, 8 (2013) 7414.
13. K.Parameswari, S.Rekha, S.Chitra and E.Kayalvizhy, *Electrochem Acta.*, 28 (2010) DOI: 10.4152/pea.201003189.
14. N.P.Dasari, B.Ganga Rao, E.Sambasiva Rao, T.M.Rao and V.S. Raneeth, *Medicinal chemistry and drug discovery.*, 3 (2012) 58.
15. P.Muthukrishnan, B.Jeyprabha and P. Prakash, *Int J Ind chem.*, 5 (2014) 5:0005-0009.
16. X.Wang, H. Yang and F.Wang, *Corros Sci.*, 52 (2010) 1268.
17. A.A.El Maghraby and Y.T.Soror, *Advances in Applied Science Research.*, 1(2010) 143.
18. M.N.Desai, S.M.Desai, M.H.Gandhi and C.B.Shah, *Int J Electrochem Sci.*, 8 (2013) 6513.
19. J.Uhera and K.Aramaki, *J Electrochem Soc.*, 138 (1991) 3245.
20. S.R.Abdel Hameed, H.I.Al-Shafey, A.S.Abul Magd and H.A.Shehata, *J Mater Environ Sci.*, 3 (2) (2012) 294.
21. M.Ozcan, F.Karadag and I.Deheri, *Acta Phys Chim Sin.*, 24 (2008) 1387.
22. M.Ozcan, R.Solmaz, G.Kardas and I.Deheri, *Surf A.*, 325 (2008) 57.
23. D.Ali, R.Solmaz, M.Ozcan and G.Kardas, *Corros Sci.*, 53 (2011) 2902.
24. X.Li, S.Deng and H.Fu, *Int J Electrochem Sci.* 8 (2013) 9201.
25. L.X.Deng and H.Fu, *Res Chem Intermed.*, 39 (2013) 1049.
26. C.Verma, M.A.Quraishi and E.E.Ebenso, *Int J Electrochem Sci.*, 8 (2013) 7401
27. A.S.Patel, V.A.Panchal, P.T.Trivedi and N.K.Shah, *Organic Schiff* 30 (2012) 3163.
28. A.Y.Musa, A.A.H.Kadhun, A.B.Mohamad and M.S.Takriff, *J Cent South Univ Technol.*, 17 (2010) 34.
29. I.B.Obot, S.A.Umoren and N.O.Obi-Egbedi, *J Mater Environ Sci*, 2 (2011) 60.
30. T.H.Ibrahim and M.Habbab, *Int J Electrochem Sci.*, 6 (2011) 5357.
31. K.P.Vinod kumar, M.S.Narayanan pillai and G.Rexin Thusnavis, *Portug Electrochim Acta.*, 28 (6) (2010) 373.
32. G.Avci, *Physicochem Eng Aspects.*, 317 (2008) 730.
33. O.K.Abiola, *Corros Sci.*, 52 (2010) 661.
34. L.A.Nnanna, O.C.Nwadiuk, N.D.Ekekwe, EP.Eti and K.B.Okeoma., *Appl. Sci Res.*, 3 (2011) 68.
35. N.Lahhit, A.Bouyanzer, J.M.Desjobert, B.Hammouti and R.Salghi, *Electrochim Acta.*, 29 (2011) 127.
36. W.A.W.Elyn Amira, A.A.Rahim, H.Osman, K.Awang and P.Bothi Raja, *Int J Electrochem Sci.*, 6 (2011) 2998.
37. K.P.Vinod Kumar, M.S.Narayanan Pillai and G.Rexin Thusnavis, *Electrochim. Acta.*, 28 (2010) 373.
38. S.S.De Assuncao Araujo Pereira, M.M.Pegas, T.L.Fernandez, M.Magalhaes, T.G.Schontag, D.C.Lago, L.F.De Senna and E.D.Elia, *Corros Sci.*, 65 (2012) 360.
39. K.Olusegun, E.M.Abiola Odin, Olowoyo and T.A.Adeloye, *Chem Soc Ethiop.*, 25 (2011) 475.
40. C.Akalezi, C.Enenebaku, B.Okolue, E.Oguzie, *Der Pharma Chemica.*, 4 (2012) 1195.
41. H.Ashassi-Sorkhabi and D.Seifzadeh, *Int J Electrochem Sci.*, 1 (2006) 92.

42. M.Znini, M.Bouklah, L.Majidi, S.Kharchouf and A.Aouniti, *Int J Electrochem Sci.*, 6 (2011) 691.
43. N.Gunavathy and S.C.Murugavel, *E-J Chemistry.*, 9 (2012) 487.
44. C.A. Loto, R.T.Loto and A.P.I.Popoola, *Physical Sciences.*, 6 (2011) 3689.
45. I.Taleb and H.Mehad, *Int J Electrochem Sci.*, 6 (2011) 5357.
46. D.Gingas, I.Mindru, L.A.Patron, J.M.Calderon-Moreno and L.Diamandescu, *Nanomater Bios.*, 6 (2011)1065.
47. Y.Abboudi, B.Hammouti, A.Abourrichel, A.Bennamara and H.Hannache, *Res Chem Intermed.*, 38 (2012) 1591.
48. M.G.Sethuraman, V.Aishwarya, C.Kamal and T.Jebakumar, *Arabian J Chem.*, (2012) <http://dx.doi.org/10.1016/j.arabjc.2012.10.013>.
49. Y.Abboudi, B.Hammouti, A.Abourrichel, B.Ihssane and A.Bennamara, *Int J Electrochem Sci.*, 7 (2012) 2543.
50. A.Lalitha, S.Ramesh and S.Rajeswari, *Electrochim Acta.*, 51 (2005) 47.
51. Q.Qu, S.A.Jiang, W.Bai and L.Li, *Electrochim Acta.*, 52 (2007) 6811.
52. I.Ahamed, R.Prasad and M.A.Quraishi, *Corros Sci.*, 52 (2010) 1472.
53. F.Bentiss, C.Jama, B.Mernari, H.E.Attari and L.Kadi, *Corros Sci.*, 51 (2009) 1628.
54. M.Elaiyachy, A.E.Idrissi and B.Hammouti, *Corros Sci.*, 48 (2006) 2470.
55. H.D.Lece, K.C.Emregul and O.Atakol, *Corros Sci.*, 50 (2006) 1460.

© 2015 The Authors. Published by ESG (www.electrochemsci.org). This article is an open access article distributed under the terms and conditions of the Creative Commons Attribution license (<http://creativecommons.org/licenses/by/4.0/>).